energies

MDPI

Article

Effects of Water and Brine Saturation on Mechanical Property Alterations of Brown Coal

Xiaogang Zhang [1], Ranjith Pathegama Gamage [1,*], Mandadige Samintha Anne Perera [1,2] and Ashani Savinda Ranathunga [3]

[1] Deep Earth Energy Research Laboratory, Building 60, Monash University, Melbourne, VIC 3800, Australia; xiaogang.zhang@monash.edu
[2] Department of Infrastructure Engineering, Building 176, The University of Melbourne, Melbourne, VIC 3010, Australia; samintha.perera@unimelb.edu.au
[3] Department of Civil Engineering, University of Moratuwa, Moratuwa 10400, Sri Lanka; ashanis@uom.lk
* Correspondence: ranjith.pg@monash.edu; Tel.: +61-3-9905-4982

Received: 24 March 2018; Accepted: 24 April 2018; Published: 2 May 2018

Abstract: The adsorption of moisture or brine into coal causes the coal mass mechanical properties to be significantly altered, which can greatly affect the coal mining and coal seam gas extraction process. A study was therefore initiated to investigate the influence of moisture and brine saturations (5–25%) on brown coals' strength through a series of unconfined compressive strength tests, with the aid of acoustic emission, optical 3-D deformation analysis and scanning electron microscopy. According to the results, the coal mass is weakened by up to 26% upon the adsorption of moisture and water saturated samples show no crack propagation, whereas brine saturation enhances coal strength by up to 21% and delays crack propagation due to the crystallization of sodium chloride. Besides, a high brine concentration (25%) greatly improves coal mass strength but impairs the increase of Young's modulus due to its corrosive nature, which is consistent with the values of maximum strain at failure of the tested samples (3.9%, 3.1% and 3.6% for 5%, 15% and 25% brine saturated samples, respectively). In addition, because of the precipitation of sodium chloride in coal and the increase of conductivity of pore fluid, more acoustic emission signals are detected for brine saturated samples, while water saturated samples exhibit mush less acoustic release compared to the unsaturated samples.

Keywords: brown coal; mechanical properties; water saturation; brine saturation

1. Introduction

Australia abounds with coal and coalbed methane (CBM) resources, with coal accounting for 32.2% of the total energy consumption in 2014–2015, which ranks as the second largest fuel supply, while CBM makes up 18% of the total gas production on an energy content basis [1]. The mechanical properties of coal mass have been shown to have great influences on coal mining as well as coal seam gas extraction [2–5]. Many kinds of accidents can happen during coal mining process, among which coal mine outburst is one of the most catastrophic phenomena. Large volumes of CO_2 and/or CH_4 burst out suddenly and violently into coal workings due to strong stress relief, frequently resulting in heavy casualties and serious economic losses. In general, three main factors contribute to coal mine outburst, including stress condition, gas content and physic-mechanical properties of the coal mass [2,6–8], of which the mechanical properties of the coal mass is the key factor affecting outburst accidents. One of the most vital factors that determine coal mass strength is the adsorbate type and content in coal as coal may become weaker with the existence of a more reactive potential adsorbate [4].

The mechanical properties of coal mass also affect the recovery process of coalbed methane. The relatively clean-burning nature of CBM has drawn much attention for its potential to provide

energy source to a world in need of clean energy supplies. Enhanced coalbed methane (ECBM) technology, which implemented by injecting CO_2 (CO_2-ECBM) or N_2 (N_2-ECBM) or flue gas into the coal seam to replace the adsorbed CH_4, has become a promising technique to recover CBM, with less environmental pollution and higher recovery rates and CO_2-ECBM has the additional benefit of immobilizing large amounts of CO_2, which is the main greenhouse gas responsible for global warming [9,10]. However, during this process, the adsorption/desorption of gas/fluids create significant changes in the mechanical properties of coal mass. Changes in coal strength properties may occur due to gas and water sorption during the ECBM process and this leads to the reduction of coal seam permeability and recovery rates [9]. Therefore, an investigation of the changes of coal mechanical property associated with adsorbate type and content is of great significance, not only for a better understanding of the outburst phenomenon during coal mining but also for a full appreciation of coal seam permeability changes, the key factor controlling CBM recovery during the ECBM process.

To date, the effects of adsorbates on coal strength changes have received considerable attention in the research literature [3–5,11–13]. Coal mass mechanical properties can be weakened by the adsorption of a more chemically reactive adsorbate. This can be explained by the theories of Gibbs [14] and Griffith [15]. For a continuous material with a unit thickness crack, the Griffith fracture criterion gives the tensile strength σ_t which allows the crack to grow as shown in Equation (1):

$$\sigma_t = \left(\frac{2E\gamma}{\pi l}\right)^{1/2} \tag{1}$$

where E is the Young's modulus of the material, γ is the surface energy per unit crack length and l is one-half the length of the crack.

The relation between surface energy and the amount of adsorption of the adsorbate in a given phase can be expressed with Gibbs' adsorption equation, as indicated in Equation (2):

$$d\gamma = -\sum(\Gamma_i d\mu_i) \tag{2}$$

where $d\gamma$ is the surface energy change due to change of adsorbate sorption, Γ_i is the surface concentration and $d\mu_i$ is the change of chemical potential of the ith adsorbate component.

Equation (2) suggests the following circumstances can lead to the reduction of surface energy: increased concentration of the adsorbate, chemical potential increment due to any change in the sorption environment and change of adsorbate from an inactive one to a more active one with higher chemical potential. Equation (1) shows that a reduced surface energy is correlated with a reduction of the tensile stress required to form or grow a new crack. Although Equation (1) is used for tensile stress circumstances, uniaxial compression strength is influenced by tensile brittle cracking and energy exchanges, according to a number of experimental results [16]. Therefore, the Griffith criterion can be adopted for uniaxial compressive situations to examine strength alterations due to sorption effects.

A number of studies to date have concerned coal mechanical property changes as the effect of sorption, however, most studies focus on CO_2, CH_4 and N_2 sorption-induced coal strength property alteration [3–5,11,17]. However, unlike conventional gas reservoirs which generally have little moisture content, coal seams are usually saturated with ground water in situ, especially for the more hydrophilic low-rank coals such as Victorian brown coal which can hold up to 70% of water by weight [18]. It is therefore important to conduct investigations on the mechanical property changes of coal subjected to water saturation. However, few studies have been done on this subject, with the exception of Perera et al. [3], Poulsen et al. [13] and Perera et al. [4] The unconfined compressive strength and Young's modulus of coals are reduced by 14.6% and 16.2% due to water saturation, respectively, according to Perera et al. [4], who used Victorian brown coal, while black coal exhibits a much higher strength reduction with reduction in UCS of 36.3% and Young's modulus of 39.5%. However, their work only considered the complete water saturation condition, while the effect of different moisture contents in coal was not included. Furthermore, as seam water always contains a certain amount of salts,

the related research on the effect of saline water saturation on coal mechanical properties is required, however, no study to date has conducted the relevant investigations on coals although a number of studies have confirmed that the existence of saline solutions can significantly affect the mechanical properties of other rocks [19–21].

Therefore, this study intents to fill this gap by performing the relevant experimental studies on the effect of moisture content and brine saturation on the mechanical properties of coals. The salt used in the present study for brine solution saturation is sodium chloride as the chemical compositions of seam water in various parts of world share similar ingredients, with sodium and bicarbonates taking the major ion roles [22], which suggests that the same seam water type can be expected, regardless of the formation's lithology or age. In addition, chloride is the major component of seam water where the coal seam is in marine or marine-transitional formations [23]. The coal samples used in this study is brown coal because of its highly hydrophilic character and its importance to Australian energy supplies, besides, despite the fact that most current ECBM projects are implemented in deep buried coal seams where high rank coals are generally expected, studies have shown that some deep lignite formations, for example the Calver Bluff formations of the Texas Wlicox Group with a buried depth deeper than 1067 m, have the potential for undertaking the ECBM projects [24]. However, relevant studies on brown coal are scarce and the main purpose of the present study is therefore to distinguish the effects of water and brine saturation on the mechanical properties of brown coals.

2. Methodology

2.1. Sample Preparation

Brown coal samples were taken from a large coal block obtained from the Hazelwood mine at Morwell in the Latrobe Valley, south-east Victoria, Australia. Two coal seams, Morwell 1 coal seam and Morwell 2 coal seam which are separated by an interlayer of sand and clay occur below the overburden that ranges from 9 to 16 m. Morwell 1 coal seam is the upper seam with the thickness up to 135 m, from which the coal samples used in this study are harvested. A 15–25 m thick aquifer lies beneath the Morwell 1 coal seam in the separating layer between the Morwell 1 and Morwell 2 coal seams [25]. An approximate analysis of the coal sample is summarised in Table 1. Large coal blocks were placed in polyethylene bags and tightly sealed immediately after being gathered from the coal mine and stored in a fog room in the Monash University Deep Earth Energy Research Laboratory (DEERL, http://www.3gdeep.com) to avoid moisture loss.

Table 1. Approximate analysis of Latrobe Valley brown coal.

Property	Values
Rank	Lignite (low rank)
Coal density (g/cm^3)	1.105
Moisture content (% wb)	55–65
Ash yield (% db)	1.7
Volatile matter (% db)	50.3
Sulphur content (% db)	0.28

wb = wet basis, db = dry basis.

Samples used in this experiment are 38 mm in diameter and 76 mm in length, in accordance with the required experimental standard [26]. First, the coal samples were cored using a 38 mm diamond-tipped bit coring machine and cut to approximately 80 mm in length using a LECO cutting machine available at DEERL. Next, the cored samples were fixed on the base of a diamond-tipped grinding machine for grinding. The grinding process began with grinding one face of the sample to completely smooth, then rotating the base to grind the other face until the sample length was reduced to approximate 76 mm. Moving the base instead of directly rotating the sample guaranteed

both faces were parallel to each other, therefore ensured that the stress applied on the specimen during the uniaxial compression test was uniformly distributed across the face. Great cares were taken when selecting the sample for the experiment to minimize the heterogeneity of the coal samples. First, samples were visually examined after grinding and those with no apparent fractures were selected; then the weight of the selected coal samples were checked and samples which are either too heavy (>98 g) or too light (<92 g) were eliminated. The remaining samples were selected for the experiment. Samples were then double-wrapped with polyethylene film and sealed in a plastic box and stored in a fog room in an attempt to prevent natural moisture loss and any change of physical and chemical properties.

2.1.1. Unsaturated Samples

Prior to preparing the unsaturated samples, it is important to determine their moisture content, because the moisture content of coal may vary during transportation, cutting and coring processes. Therefore, three small natural coal blocks taken from the same large coal block from which the coal samples were made were weighed before putting them in the oven and the temperature was set to 105 °C. The weights of these three blocks were recorded with time until the values remained constant. The moisture content of each block was then calculated, which are 57.1%, 57.8% and 57.0%, respectively, as shown in Table 2. The coal sample used in this study was assumed to have a moisture content of 55–65%, which indicates that the influences from the external environment on the moisture content of natural coal sample were minimal.

Table 2. Moisture content in natural samples.

Block No.	1	2	3
Initial weight (g)	19.8	37.2	82.6
Dry weight (g)	8.5	15.7	35.6
Moisture content (%)	57.1	57.8	57.0
Average moisture content (%)		57.3	

2.1.2. Water Saturation Samples

Three pre-weighed samples were put in a desiccator filled with de-ionised water. A vacuum pump was connected to the desiccator and ran for 20 min until the desiccator was fully sealed. The desiccator was then left for 24 h. After that, samples were taken out and weighed to determine how much moisture the samples had adsorbed. The samples were then put back into the desiccator for another 24 h to gain further moisture and the weight of each sample was re-checked. This procedure was repeated several times until the weight of each specimen remained constant, indicating that the complete water saturation had been achieved. Polyethylene film was used again for covering the water saturated samples and the UCS tests were conducted within 20 min after the samples were removed from the desiccator to minimise any change to the saturation state.

2.1.3. Low Moisture Content Samples

For low moisture content sample preparation, three pre-weighed natural samples were kept in room environment (around 20 °C) for 12 h to allow evaporation to occur. Samples were then weighed to determine the amount of moisture evaporated. The moisture content of these three samples was calculated as listed in Table 3. The samples were then enclosed with polyethylene film and stored in the fog room for two weeks to allow the disturbed moisture distribution to be evenly distributed prior to testing. The authors attempted to prepare dry samples in order to produce low moisture content samples. Samples with 25 mm in diameter and 50 mm in length were placed in the oven with the temperature being set to 30 °C. A low temperature was selected as low-rank coal is much weaker in terms of mechanical strength than high-rank coal and a high temperature environment can create

a sudden decrease of moisture content, which may lead to great alterations in the coal mechanical properties. However, many fractures still formed in the samples during the drying process even under this low drying temperature, as shown in Figure 1.

Table 3. Low moisture content samples.

Sample No.	L-01	L-02	L-03
Initial weight (g)	95.8	95.0	94.0
Final weight (g)	75.8	73.6	72.7
Moisture content (%)	46.0	44.9	44.8
Average moisture content (%)		45.2	

Figure 1. Fractures after low-temperature drying.

2.1.4. Brine Saturation Samples

The salinity of seam water can be expressed as the total dissolved solids in seam water. Normally, the salt content of coal seam water varies widely in different places; in some places where shallow coal seams exist, the salinity of seam water can be as low as that of fresh water (10–500 mg/L) as a result of exposure to fresh groundwater recharge, while for coal seam associated with high salinity environment the salt concentration can reach up to ten times higher than that of seawater (300,000 mg/L) [27]. Therefore, in the present study, 5%, 15% and 25% NaCl concentration solutions were prepared for the brine saturation. The same procedures for complete water saturation were followed to obtain complete brine saturation samples. The brine saturated samples were then taken out from the desiccator, wrapped with polyethylene film and tested within 20 min to minimise the external interferences in samples.

In total, three different moisture conditions and three different brine saturation conditions were prepared for this study, as summarised in Table 4.

Table 4. Experimental plan.

Experimental Condition	Number of Samples
Low moisture content (45.2%)	3
Unsaturated sample (57.3%)	3
Water saturation (65.0%)	3
5% NaCl saturation	3
15% NaCl saturation	3
25% NaCl saturation	3

2.2. Experimental Techniques

UCS tests were conducted within 20 min of each sample achieving the corresponding saturation condition and were performed using the Shimadzu compression machine (AG-300kNXplus,

Shimadzu Corporation, Kyoto, Japan) available at DEERL. The high precision force measurement of this compression tester can ensure the error of the recorded force data is within ±0.5% of the indicated test force. The compression loading rate was set to 0.1 mm/min. The applied load on the samples was monitored by an advanced data acquisition system as a function of time. A non-contact optical 3-D deformation measuring system (ARAMIS photogrammetry) was adopted to measure the corresponding strains during the strength tests and an acoustic emission (AE) system was used for recording fracture propagation during sample compression. A detailed description of ARAMIS and the AE system can be found in Rananthunga et al. [5].

Scanning electron microscopy (SEM) analysis and energy-dispersive X-ray (EDX) analysis were used for the complete SEM and EDX analysis of coal samples before and after water and brine saturation. During the sample preparation process, several slices around 3 mm thick were cut from the same block and saturated in the desiccator together with all the other samples. These small blocks were then taken out after the corresponding saturation and grounded into coarse powders (around 0.5 mm in diameter) for SEM/EDX analysis. Since the brown coal used in this study has poor conductivity, coarse powder was used instead of slices to avoid sample charging, which can cause many unusual side-effects such as image distortions. SEM/EDX analysis was performed at the Monash Centre for Electron Microscopy (MCEM) using the FEI Quanta 3D FEG FIB facility. Five sessions were conducted: unsaturated sample; water-saturated sample; sample with 5% NaCl saturation; sample with 15% NaCl saturation; and sample with 25% NaCl saturation. Unsaturated samples acted as the reference and coal structure alterations were obtained from SEM results.

3. Results and Discussion

A total of 18 samples were tested in this study. The uniaxial compressive strength and Young's modulus of each sample were recorded and calculated. The AE responses and ARAMIS images were analysed and the alteration of the micro-structure of each sample was displayed by the representative SEM images. Table 5 gives the UCS and Young's modulus values of all the samples tested in this study. Since the UCS deviations of the three samples under each experimental condition were minimal, for discussion purposes, the sample with the lowest UCS values was selected to represent each condition. The representative stress-strain curves of the tested sample under each saturation condition are given in Figure 2.

Table 5. Uniaxial compressive strength (UCS) and Young's modulus (E) of all samples and comparison of these values with values of unsaturated samples.

Sample Description	UCS (MPa)	Average UCS (MPa)	ΔUCS (%)	E (MPa)	Average E (MPa)	ΔE (%)
Unsaturated (57.3%)	1.15	1.13	-	40	38	-
	1.12	-	-	38	-	-
	1.11	-	-	36	-	
Low moisture (45.2%)	1.28	1.25	+11	43	42	+11
	1.23	-	-	42	-	-
	1.24	-	-	41	-	
Water-saturated (65%)	0.82	0.84	−26	35	35	−9
	0.86	-	-	33	-	-
	0.85	-	-	36	-	-
5% NaCl	1.19	1.20	+6	54	53	+40
	1.22	-	-	51	-	-
	1.18	-	-	54	-	-
15% NaCl	1.25	1.24	+10	67	65	+71
	1.21	-	-	63	-	-
	1.27	-	-	64	-	-
25% NaCl	1.37	1.37	+21	51	53	+41
	1.40	-	-	51	-	-
	1.35	-	-	59	-	-

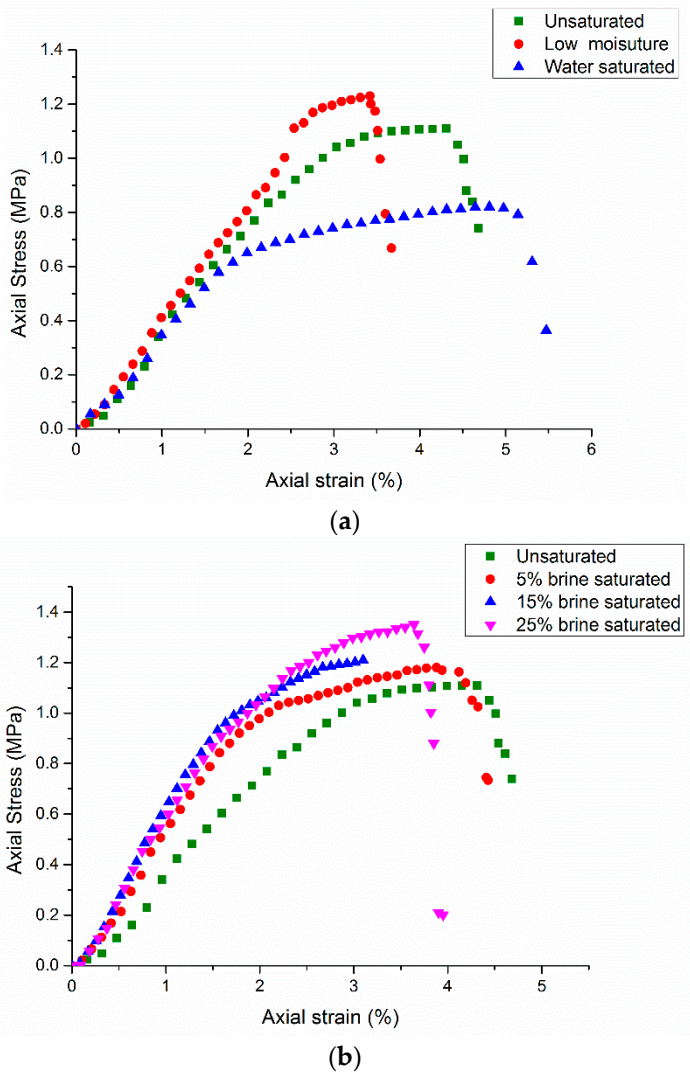

Figure 2. Axial stress versus strain curves of (**a**) unsaturated sample, low moisture content sample and water saturated sample; (**b**) unsaturated sample, 5%, 15%, 25% brine saturated sample.

3.1. Uniaxial Compressive Strength (UCS) Analysis

3.1.1. Moisture Content Effect on UCS

According to Table 5, the UCS value of brown coal samples reduces with the increase of moisture content in the coal mass. The water-saturated sample has the lowest UCS value of 0.82 MPa compared to the unsaturated sample which has the value of 1.11 MPa, while the sample with low moisture content exhibits the highest strength with the UCS value of 1.23 MPa. Compared to unsaturated samples, the average UCS reduction for water-saturated samples is 26%, while an average UCS increment of 11% is observed in low moisture samples.

This phenomenon of high moisture content with low mechanical strength can be expected, since water is one of the most determinant factors for the mechanical properties of any rock type [3], including coal. The adsorption of a more chemically reactive adsorbate can result in a weakened coal mass and water molecules are preferably adsorbed onto the polar sites in coal microstructure surfaces [28], forming water clusters induced by hydrogen bonding between water molecules. This indicates that: (1) the previous void volumes of coal pores are now occupied by the more chemically reactive adsorbates (water molecules) and (2) the concentration of the adsorbate (water molecules) increases with the adsorption of water molecules. Furthermore, with water-dispersed

interaction in coal, the coal structure can be rearranged to some extent, because of the polymeric nature of coal as well as the presence of functional groups which results in the interaction between the adsorbed water molecules and the solids [29]. All these processes lead to the reduction of surface energy, which reduces coal mass strength according to Equations (1) and (2). Moreover, corrosive deterioration induced by water saturation leads to the reduction of the strength of the coal mass. Some minerals in coal dissolved in water to some extent during water saturation and the coal mass is therefore weakened due to the loss of these minerals. This can be further confirmed by the SEM images of microstructure changes of coal samples as shown in Figure 3.

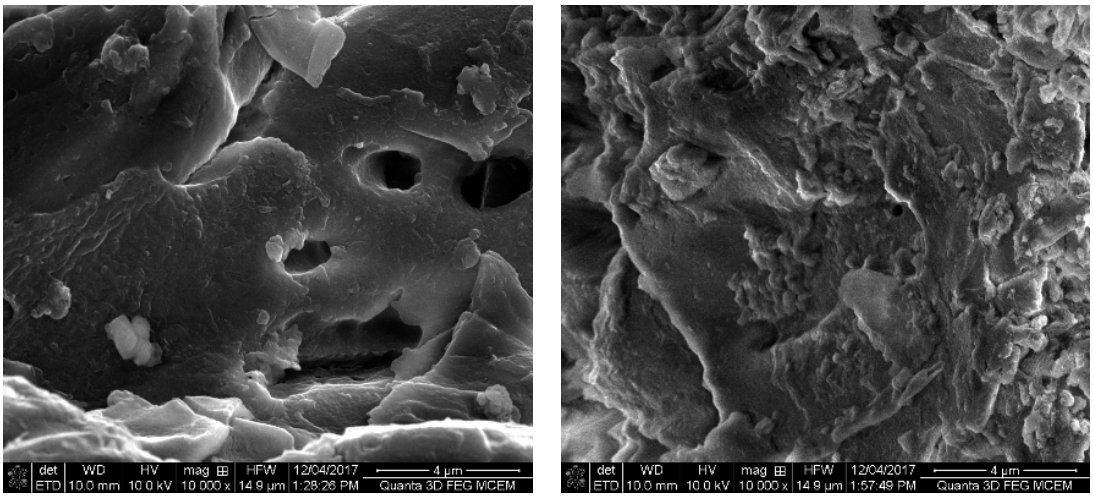

(**a**) (**b**)

Figure 3. Scanning electron microscopy (SEM) images of (**a**) unsaturated and (**b**) water-saturated samples (Images taken under accelerated voltage of 10 kV, 47 pA probe current and magnification of 10,000×; unsaturated sample exhibit a much smoother surface with larger pores while water saturated sample shows a relatively lumpy surface with small pores).

Perera et al. [4] also performed UCS tests using samples of black and brown coal subjected to water saturation. Experimental data obtained from the present study and that of Perera et al. [4] are displayed in Table 6. Compared to the experimental data obtained by Perera et al. [4], the UCS reduction of brown coal after water saturation in the present study is much less than that reported in Perera et al. [4] (26% for brown coal versus 36% for black coal). An explanation for this phenomenon can be that black coals have much longer and more complicated coalification process than brown coals, leaving black coals with more fractures accompanied with well-developed cleat systems. This well-developed cleat system in black coal can provide more places catering water molecules and these water molecules cause fractures in coal to expand by moving towards the tips of fractures, which induces stress concentrations at the tips [4], weakening the overall strength of the coal mass. This also explains the fact that the average UCS reduction (26%) of the brown coal sample after water saturation in the present study was higher than the average UCS reduction (15%) of the brown coal sample after water saturation in Perera et al. [4]. The brown coal samples used in both studies were harvested from the same coal mine but different blocks, the micro-structure of these two coals therefore can vary significantly. This can be confirmed by the average UCS value of the unsaturated samples, the average UCS value of the unsaturated samples in the present study is much lower than those in Perera et al. [4], which suggests that the brown coal samples used here have more fractures than the brown coals used in Perera et al. [4]. Therefore, higher strength reduction in the present study after water saturation can be expected than that reported by Perera et al. [4].

Table 6. Comparison of UCS values in present study and Perera et al.

Coal type	Brown Coal	Brown Coal	Black Coal
Average UCS for unsaturated samples (MPa)	1.13	2.36	32.00
Average UCS for water-saturated samples (MPa)	0.84	2.04	20.95
ΔUCS (%)	−26	−15	−36
Reference	-	Perera et al. [4]	Perera et al. [4]

3.1.2. Brine Content Effect on UCS

As indicated in Table 5, the UCS values of all the brine-saturated samples increased compared to the UCS values of the unsaturated samples and the increment between unsaturated and brine-saturated samples increases as the concentration of brine solution rises. Table 5 shows the average UCS increments of 5%, 15% and 25% brine-saturated samples compared with those of unsaturated samples are 6%, 10% and 21%, respectively.

As discussed in Section 3.1.1, after water saturation brown coal samples are significantly weakened in terms of UCS values, however, brine saturated samples show higher UCS values than water-saturated samples and unsaturated samples, which indicates that the sodium chloride solution may somehow strengthen the coal mass. This is the result of the crystallisation of NaCl in the pores of the coal sample during brine saturation. Samples adsorbed water molecules and Na^+, Cl^- at the same time and the adsorbed cations and anions crystallized inside the coal mass, contributing to the increase of coal sample strength by reducing the number of voids as well as increasing the resistance during the compression test [20]. Figure 4 provides the evidence of the sodium chloride crystals in coal sample. In addition, the amounts of minerals dissolved in brine are decreased due to the presence of cations and anions, which alleviates strength reduction due to mineral dissolution.

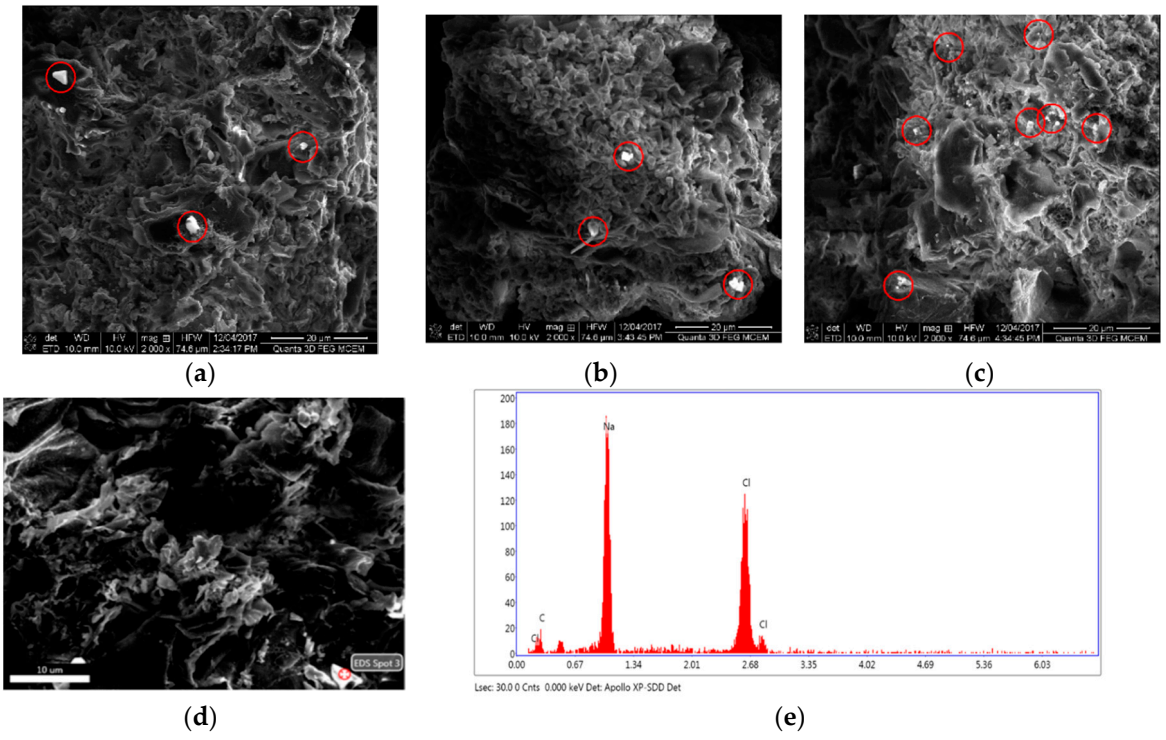

Figure 4. SEM images of (**a**) 5%, (**b**) 15% and (**c**) 25% brine-saturated samples (White crystals inside the red circles are NaCl crystals. Images were taken under accelerated voltage of 10 kV, with 47 pA probe current and magnification of 2000×) (**d**), (**e**) Energy dispersive X-ray spectroscopy (EDS) analysis of precipitated white crystals.

5% brine saturation samples and 15% brine saturation samples achieve average UCS increments of 6% and 10%, respectively, compared to unsaturated samples. However, this increment increases to 21% for 25% brine-saturated samples. The followings can explain this pronounced increase of UCS values for 25% brine-saturated samples: (1) fewer minerals dissolved in the brine solution since a high salinity solution significantly limits the amount of mineral in coal that is able to dissolve in the brine solution, which eases the strength reduction induced by mineral dissolution; (2) more NaCl molecules crystallized in the coal, adding more strength to the coal mass. As the mass fraction of a fully-saturated NaCl solution is around 26.47% at room temperature (20 °C), the 25% NaCl brine solution used in the present study has nearly the maximum amount of NaCl that is able to be dissolved in water. Compared to low-salinity solutions (5%, 15%), which still have relative high potential to digest NaCl, the amount of NaCl crystallized in the coal mass is relatively small; high salinity solution (25%) provides more cations and anions that can be precipitated in the coal mass, adding to its strength. SEM images of Figure 4 shows that under the same viewing area, the amount of sodium chloride precipitated in the coal structure for 25% brine-saturated samples is much greater than that of 5% brine-saturated and 15% brine-saturated samples.

3.2. Young's Modulus Analysis

Young's modulus represents the stiffness of materials and shows the ability of a material to resist deformation under loading [30]. The Young's modulus of each sample, average Young's modulus of each saturation condition and a comparison of Young's modulus between each saturation condition and unsaturated samples are listed in Table 5. All the Young's moduli were calculated using data from the elastic regions of stress-strain curves during monotonous loading.

3.2.1. Moisture Content Effect on Young's Modulus

As indicated in Table 5, the average Young's modulus for low moisture samples, unsaturated samples and water-saturated samples are 42 MPa, 38 MPa and 35 MPa, respectively. This indicates that coal Young's modulus decreases with increasing moisture content in coal. A reduction of Young's modulus of a material exhibits an enhancement of its ductile behaviour, therefore the ductile properties of the coal samples improved with the increase of the moisture content in coal. Larsen et al. [31] states that the natural coal mass possesses strained and glassy features and coal matrix swelling can convert this strained state to a more relaxed state. This state transfer is due to the rearrangement of coal structure from a high-energy state to a low-energy and more significantly non-covalently-related state. In this case, coal matrix swelling is induced by the adsorption of water molecules and literatures have reported that coal swells near-linearly with the increase of the moisture content [32,33], therefore the increased moisture content in coal leads to a higher structure rearrangement (as shown in Figure 3) which results in the improvement of the ductile behaviour. Besides, as water is a polar molecule, the polar nature of water molecules perplexes the interactions between water and coal macerals and mineral matters; Figure 3 shows that the surface roughness of the coal has changed upon the adsorption of moisture, some literatures have demonstrated that the changes in the surface roughness due to the adsorption of fluids on coal lead to a reduced Young's modules by enhancing the normal stress transported across the cleats [34,35]. Furthermore, the existence of free water within the coal assists the sliding of initial cracks during compression by reducing the friction forces between the initial cracks [36], which also contributes to the improvement of the coal ductile properties.

3.2.2. Brine Content Effect on Young's Modulus

Table 5 shows that the Young's moduli of all the samples are significantly increased after brine saturation. The average increments of Young's modulus for brine-saturated samples are 40% (5% brine), 71% (15% brine) and 41% (25% brine), respectively, compared with unsaturated samples. Coal mass stiffness is enhanced after brine saturation because of the previously-mentioned crystallization of

sodium chloride in the coal mass. Cracks are initiated during compression within coal samples and the NaCl crystals inside coal mass increases the friction force between crack surfaces, resulting in more resistance of crack development during the crack initiation process. This reduces the plasticization capacity of the coal mass, contributing to the increase of Young's modulus. These influences are more significant with the increase of NaCl concentration, since samples with 15% brine saturation exhibit much higher Young's moduli compared to samples saturated with 5% brine. However, it is interesting to note that the average Young's modulus of the 25% brine saturated samples is about the same as that of 5% brine saturated samples, which indicates that the variation of Young's modulus under brine saturation may follow a parabolic fashion with the increase of NaCl concentration. This is due to the chemical corrosive nature of brine solutions as indicated by Feng et al. [37]. The corrosive effect of the NaCl ions may improve the plasticization of the coal during the interaction between the ions and the coal mass and this corrosive effect is more significant when samples are soaked with high NaCl concentration solutions. As shown in Figure 5, the microstructures of brine-saturated samples are greatly altered compared to the unsaturated sample shown in Figure 3a, especially for the 25% brine-saturated sample. In general, coal mass stiffness is enhanced with NaCl crystallization, while coal mass ductility is improved by the corrosive nature of brine. The stiffness gained due to NaCl deposits in coal is more profound than the corrosive effect of brine on coal mass ductility when there is a low NaCl concentration, while for high NaCl concentration saturation, the ductility increment induced by brine corrosion is much more enhanced compared to the low NaCl concentration saturation.

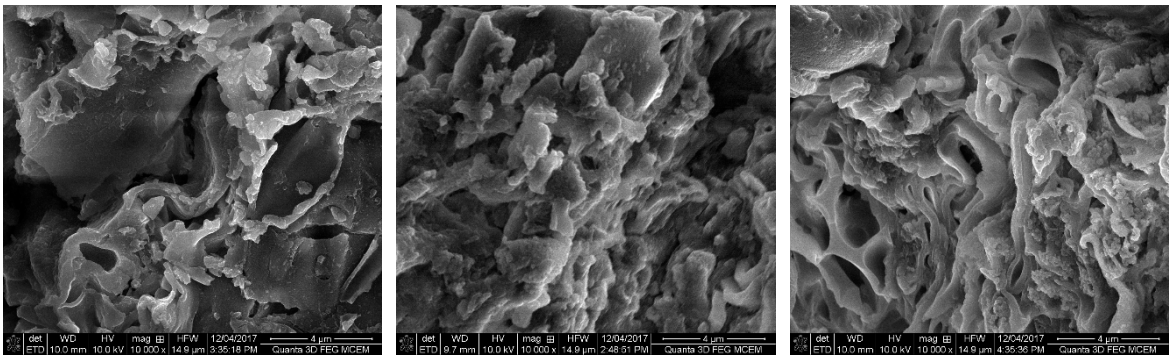

(**a**) (**b**) (**c**)

Figure 5. SEM images of (**a**) 5%, (**b**) 15% and (**c**) 25% brine-saturated samples (Images taken under accelerated voltage of 10 kV, with 47 pA probe current and magnification of 10,000×; more flaky textures and pores are presented in these images due to the corrosion of brine solution).

3.3. Strain Results

The failure patterns of samples under different conditions during compression were captured using ARAMIS photogrammetry, as shown in Figure 6. All the pictures display sample states at failure under loading.

3.3.1. Moisture Content Effect on Strain Behaviour

As shown in Figure 6, the ductile properties of coal mass are improved as the maximum strain at failure increases with the increasing moisture content in coal. In addition, failure patterns of the sample suggest that the low moisture content sample presents a splitting failure pattern, while the unsaturated sample failed along major cleats and the water-saturated sample failed along major and minor cleats. This indicates the heterogeneous nature of water saturated samples compared with the unsaturated sample, which is relatively more homogenous with a general strain distribution.

3.3.2. Brine Content Effect on Strain Behaviour

According to Figure 6, samples subjected to 15% brine saturation are highly brittle in nature with an evident shear-dominated failure, while samples with 5% and 25% brine saturation exhibit ductile behaviour to some extent with failure along major cleats (for the 5% brine-saturated sample) and major and minor cleats (for the 25% brine-saturated sample). This is consistent with the analysis of the Young's modulus in Section 3.2.2, with the highest Young's modulus shown by the 15% brine saturated samples. Coal stiffness is enhanced in the context of increasing brine concentration to a certain degree and then abated by further increasing the brine concentration. Furthermore, Rathnaweera et al. [20] suggest that the NaCl crystals within the pore spaces can result in the expansion of coal pores. The crystalized NaCls squeeze the pore walls, making them thinner and weaker and this phenomenon is more significant for samples saturated with high brine concentration solution, therefore many weak zones may form in brine-saturated samples with high concentrations during the loading process.

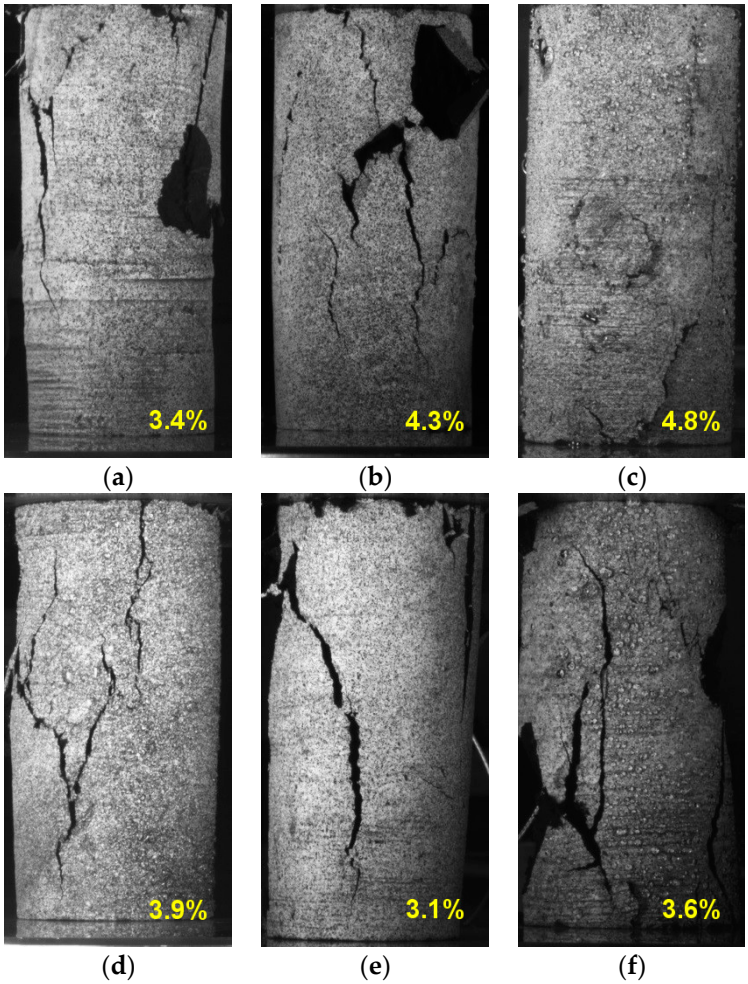

Figure 6. Sample appearance at failure of tested samples ((**a**) low moisture, (**b**) unsaturated, (**c**) water saturated, (**d**) 5% brine saturated, (**e**) 15% brine saturated and (**f**) 25% brine saturated. Yellow figures denote the respective maximum strains at failure for each condition).

3.4. Fracture Propagation

An acoustic emission (AE) system was adopted to identify the fracture development behaviours of brown coal samples subjected to various saturation conditions during loading. Fracture development can be displayed by the cumulative number of AE counts, which represent the energy released during fracture propagation during sample compression [38]. At the beginning of compression, cracks within

the coal mass are closed which is identified as the crack closure stage and this stage starts from the very beginning of loading until the stress reaches crack initiation stress (σ_{ci}). The sample then enters the stable crack propagation stage, during which the increasing compressive stress causes minor damage accompanied by a slight increase in the cumulative number of AE counts, which is represented within the period from the crack initiation stress (σ_{ci}) to crack damage stress (σ_{cd}). Further increase of compression causes unstable crack development, with a marked increase of cumulative AE counts as the failure plane is damaged with the increase of axial stress. Load application during this stage causes significant damage to the coal mass until the sample fails.

Tables 7 and 8 give the stress threshold values of the tested samples under various conditions from AE data and Figure 7 shows the comparison of the cumulative number of AE counts with axial stress for the tested samples.

Table 7. Stress threshold values of different moisture content samples.

Conditions	cis (MPa)	cds (MPa)	UCS (MPa)
Low moisture (45.2%)	0.75	1.14	1.23
Unsaturated (57.3%)	0.31	0.52	1.11
Water saturated (65%)	-	-	0.82

cis: crack initiation stress; cds: crack damage stress.

Table 8. Stress threshold values of brine-saturated samples.

Conditions	cis (MPa)	cds (MPa)	UCS (MPa)
5%	0.37	0.64	1.18
15%	0.58	0.82	1.21
25%	0.84	0.99	1.35

cis: crack initiation stress; cds: crack damage stress.

As indicated in Figure 7a and Table 7, low moisture content samples and unsaturated samples show remarkable cracking behaviours, with all three stages being clearly presented. During the compression process, the crack closure region appears first, without any acoustic emission counts. The samples then enter the stable crack propagation stage, with a stable increase of acoustic emission counts indicating a nearly linear release of strain energy. Unstable crack propagation begins when the load reaches crack damage stress and during this process, samples are damaged by loading until they eventually fail with the exponential increase of strain energy release as shown in Figure 7a. However, water-saturated sample exhibits a different crack propagation pattern. Without stable and unstable crack propagation processes, the AE system can only detect acoustic emissions when a sample fails, as the sample reveals failure immediately after the crack closure stage. This is because brown coal samples are significantly weakened after water saturation. As mentioned previously, the adsorption of water into the coal mass impairs the tips of fractures in the coal, which greatly weakens these fractures. The weakened fractures can fail without any crack propagation process during loading.

Figure 7b shows the variation of AE cumulative counts for brine-saturated samples, which suggests that the cumulative counts increase with the increase of brine concentration. This is because the amount of sodium chloride crystals that precipitated inside coal sample increases with the increasing brine concentration. During compression, these sodium chloride crystals in the coal sample are crushed, which releases additional AE energies. In addition, the conductivity of fluids in the coal sample is increased with the increase of free cations and anions, the increase of brine conductivity leads to the enhanced ability of AE sensors to detect relatively smaller energy emissions which are not be able to be captured by the sensors in low conductive media, therefore allowing brine to deliver more energy generated during crack propagation. Table 8 shows the variation of stress threshold values of brine-saturated samples. A clear increase of crack initiation stress and crack damage stress can be

observed. This indicates that, with the increase of brine concentration, more energies are required to reach the corresponding stages, which further confirms that coal mass strength is enhanced with the increase of brine concentration. The crystallization of NaCl plays an important role in the increment of coal mass strength, since the pre-existing voids in the coal mass are filled with the NaCl crystals after brine saturation, which raises the energy required for fracture development.

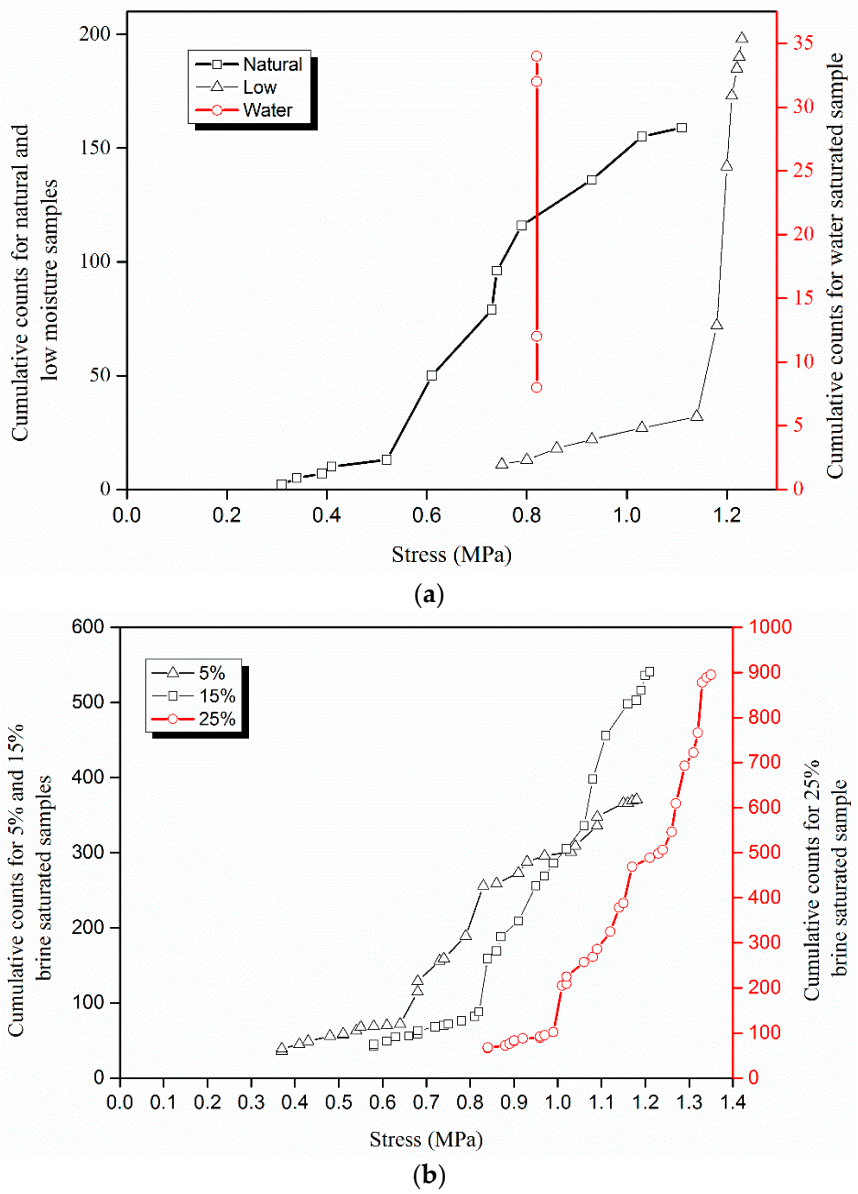

Figure 7. (**a**) Comparison of cumulative number of acoustic emission (AE) counts for different moisture content samples; (**b**) Comparison of cumulative number of AE counts for different brine content samples.

4. Conclusions

A laboratory study was carried out to characterise the influences of moisture and brine saturation on brown coal's mechanical attributes through a UCS testing programme. The following major conclusions can be drawn from the experimental results:

- The adsorption of moisture into coal causes the UCS values of brown coal to be reduced by up to 26% due to the structure rearrangement of coal upon the interaction between water molecules and coal. The SEM results further confirmed the associated microstructure alterations.
- Brine-saturated samples exhibit an increase in UCS values by up to 21% compared to unsaturated samples due to the crystallisation of sodium chloride in coal that can be observed in SEM images. 25% brine-saturated samples show a pronounced increase of UCS values (21%) compared to 5% brine-saturated samples (6%) and 15% brine-saturated samples (10%). The much higher precipitation ability of sodium chloride of 25% NaCl solution which is nearly fully-saturated at room temperature is the main reason for this marked UCS increment. The decrease of mineral dissolution due to high salinity environment further contributes to the reduction of coal mass strength deterioration.
- An increase in Young's modulus of 40%, 71% and 41% for 5%, 15% and 25% brine-saturated samples was obtained, respectively. Coal mass stiffness is enhanced due to the crystallization of sodium chloride in the coal mass; however, a reduction of the increase of Young's modulus for 25% saturated samples was observed. This is because that the corrosive effect of the brine solution is enhanced for high sodium chloride concentrations, adding to sample's ductility. This phenomenon is in accordance with the maximum strains at failure for brine-saturated samples obtained from ARAMIS results, which are 3.9%, 3.1% and 3.6% for 5%, 15% and 25% brine saturated samples, respectively.
- In addition, unsaturated samples and low moisture samples show a clear crack development process, while for water-saturated sample acoustic emissions can only be detected when the sample fails due to the fact that the samples have already been significantly weakened after water saturation.
- The brine-saturated samples show delays during the crack propagation process. The AE signals for brine-saturated samples increase with the increase of brine concentration because of the increasing numbers of NaCl crystals precipitated within coal, as well as the increased transferability of acoustic signal with the presence of brine solution in pore fluid.

Author Contributions: Xiaogang Zhang performed the experiment, analysed the data, prepared the draft manuscript and revised the manuscrip. Ranjith Pathegama Gamage mentored the experiment and reviewed the draft. Mandadige Samintha Anne Perera made important suggestions and recommendations, Ashani Savinda Ranathunga helped prepared the samples and made important recommendations.

Acknowledgments: The authors acknowledge use of the facilities and the assistance of Xiya Fang at the Monash Centre for Electron Microscopy. This research used equipment funded by Australian Research Council grant (LE0882821). We thank the anonymous reviewers for their careful reading of our manuscript and their many insightful comments. Xiaogang Zhang would like to acknowledge the financial support from the China Scholarship Council and Faculty of Engineering, Monash University.

Conflicts of Interest: The authors declare no conflict of interest.

References

1. Department of Industry, Innovation and Science Unconventional Gas. Available online: https://industry.gov.au/resource/UpstreamPetroleum/Pages/UnconventionalGas.aspx (accessed on 10 December 2017).
2. Zhi, S.; Elsworth, D. The Role of gas desorption on gas outbursts in underground mining of coal. *Geomech. Geophys. Geo-Energy Geo-Resour.* **2016**, *2*, 151–171. [CrossRef]
3. Perera, M.; Ranjith, P.; Peter, M. Effects of saturation medium and pressure on strength parameters of Latrobe Valley brown coal: Carbon dioxide, water and nitrogen saturations. *Energy* **2011**, *36*, 6941–6947. [CrossRef]
4. Perera, M.S.A.; Ranathunga, A.S.; Ranjith, P.G. Effect of Coal Rank on Various Fluid Saturations Creating Mechanical Property Alterations Using Australian Coals. *Energies* **2016**, *9*, 440. [CrossRef]
5. Ranathunga, A.; Perera, M.; Ranjith, P.; Bui, H. Super-critical CO_2 saturation-induced mechanical property alterations in low rank coal: An experimental study. *J. Supercrit. Fluids* **2016**, *109*, 134–140. [CrossRef]

6. Beamish, B.B.; Crosdale, P.J. Instantaneous outbursts in underground coal mines: An overview and association with coal type. *Int. J. Coal Geol.* **1998**, *35*, 27–55. [CrossRef]
7. Zhao, H.; Kaunda, R.B. Numerical Assessment of the Influences of Gas Pressure on Coal Burst Liability. *Energies* **2018**, *11*, 260. [CrossRef]
8. Wang, F.; Zhang, C.; Liang, N. Gas Permeability Evolution Mechanism and Comprehensive Gas Drainage Technology for Thin Coal Seam Mining. *Energies* **2017**, *10*, 1382. [CrossRef]
9. Zhang, X.; Ranjith, P.G.; Perera, M.S.; Ranathunga, A.; Haque, A. Gas Transportation and Enhanced Coalbed Methane Recovery Processes in Deep Coal Seams: A Review. *Energy Fuels* **2016**, *30*, 8832–8849. [CrossRef]
10. Hardisty, P.E.; Clark, T.S.; Hynes, R.G. Life cycle greenhouse gas emissions from electricity generation: A comparative analysis of Australian energy sources. *Energies* **2012**, *5*, 872–897. [CrossRef]
11. Masoudian, M.S.; Airey, D.W.; El-Zein, A. Experimental investigations on the effect of CO_2 on mechanics of coal. *Int. J. Coal Geol.* **2014**, *128*, 12–23. [CrossRef]
12. Lu, Y.; Zhou, Z.; Ge, Z.; Zhang, X.; Li, Q. Coupling effect of intruding water and inherent gas on coal strength based on the improved (mohr-coulomb) failure criterion. *Minerals* **2016**, *6*, 118. [CrossRef]
13. Poulsen, B.; Shen, B.; Williams, D.; Huddlestone-Holmes, C.; Erarslan, N.; Qin, J. Strength reduction on saturation of coal and coal measures rocks with implications for coal pillar strength. *Int. J. Rock Mech. Min. Sci.* **2014**, *71*, 41–52. [CrossRef]
14. Gibbs, J.W. On the equilibrium of heterogeneous substances. *Am. J. Sci.* **1878**, *16*, 441–458. [CrossRef]
15. Griffith, A.A. The phenomena of rupture and flow in solids. *Philos. Trans. R. Soc. Lond. A* **1921**, *221*, 163–198. [CrossRef]
16. Van Eeckhout, E.M. The mechanisms of strength reduction due to moisture in coal mine shales. *Int. J. Rock Mech. Min. Sci. Geomech. Abstr.* **1976**, *13*, 61–67. [CrossRef]
17. Espinoza, D.; Pereira, J.-M.; Vandamme, M.; Dangla, P.; Vidal-Gilbert, S. Desorption-induced shear failure of coal bed seams during gas depletion. *Int. J. Coal Geol.* **2015**, *137*, 142–151. [CrossRef]
18. Durie, R. *The Science of Victorian Brown Coal: Structure, Properties and Consequences for Utilization*; Butterworth-Heinemann: Oxford, UK, 2013.
19. Huang, Y.-H.; Yang, S.-Q.; Hall, M.R.; Zhang, Y.-C. The Effects of NaCl Concentration and Confining Pressure on Mechanical and Acoustic Behaviors of Brine-Saturated Sandstone. *Energies* **2018**, *11*, 385. [CrossRef]
20. Rathnaweera, T.; Ranjith, P.; Perera, M. Salinity-dependent strength and stress–strain characteristics of reservoir rocks in deep saline aquifers: An experimental study. *Fuel* **2014**, *122*, 1–11. [CrossRef]
21. Zhang, S.; Xian, X.; Zhou, J.; Zhang, L. Mechanical behaviour of Longmaxi black shale saturated with different fluids: An experimental study. *RSC Adv.* **2017**, *7*, 42946–42955. [CrossRef]
22. Authority, S.C. *Coal Seam Gas Impacts on Water Resources*; Sydney Catchment Authority: Sydney, Australia, 2012.
23. Van Voast, W.A. Geochemical signature of formation waters associated with coalbed methane. *Aapg Bull.* **2003**, *87*, 667–676. [CrossRef]
24. McVay, D.; Ayers Jr, W.; Jensen, J.; Garduno, J.; Hernandez, G.; Bello, R.; Ramazanova, R. *CO_2 Sequestration Potential of Texas Low-Rank Coals*; Texas Eng Experiment Station: College Station, TX, USA, 2006.
25. Fraser, C.; Pitt, H. Artesian dewatering operations at Morwell open cut. In Proceedings of the First International Mine Drainage Symposium, Denver, CO, USA, 1 May 1979; pp. 362–382.
26. *ASTM D7012-14e1, Standard Test Methods for Compressive Strength and Elastic Moduli of Intact Rock Core Specimens under Varying States of Stress and Temperatures*; ASTM International: West Conshohocken, PA, USA, 2014; Available online: www.astm.org (accessed on 15 February 2018).
27. Khan, S.; Kordek, G. *Coal Seam Gas: Produced Water and Solids*; Report commissioned for the independent review of coal seam gas activities in NSW by the NSW Chief Scientist & Engineer; School of Civil Environmental Engineering, The University of New South Wales: Sydney, Australia, 2014.
28. Day, S.; Fry, R.; Sakurovs, R. Swelling of moist coal in carbon dioxide and methane. *Int. J. Coal Geol.* **2011**, *86*, 197–203. [CrossRef]
29. Walker, P.L., Jr.; Verma, S.K.; Rivera-Utrilla, J.; Davis, A. Densities, porosities and surface areas of coal macerals as measured by their interaction with gases, vapours and liquids. *Fuel* **1988**, *67*, 1615–1623. [CrossRef]
30. Roylance, D. *Mechanical Properties of Materials*; Massachusetts Institute of Technology: Cambridge, MA, USA, 2008; pp. 51–78.

31. Larsen, J.W.; Flowers, R.A.; Hall, P.J.; Carlson, G. Structural rearrangement of strained coals. *Energy Fuels* **1997**, *11*, 998–1002. [CrossRef]
32. Liu, J.; Peach, C.J.; Spiers, C.J. Anisotropic swelling behaviour of coal matrix cubes exposed to water vapour: Effects of relative humidity and sample size. *Int. J. Coal Geol.* **2016**, *167*, 119–135. [CrossRef]
33. Pan, Z.; Connell, L.D.; Camilleri, M.; Connelly, L. Effects of matrix moisture on gas diffusion and flow in coal. *Fuel* **2010**, *89*, 3207–3217. [CrossRef]
34. Hol, S.; Gensterblum, Y.; Massarotto, P. Sorption and changes in bulk modulus of coal—Experimental evidence and governing mechanisms for CBM and ECBM applications. *Int. J. Coal Geol.* **2014**, *128*, 119–133. [CrossRef]
35. Hol, S.; Peach, C.J.; Spiers, C.J. Applied stress reduces the CO_2 sorption capacity of coal. *Int. J. Coal Geol.* **2011**, *85*, 128–142. [CrossRef]
36. Zhou, Z.-L.; Xin, C.; Yuan, Z.; Lu, C.; Xiong, C.; Li, X.-B. Strength characteristics of dry and saturated rock at different strain rates. *Trans. Nonferr. Metals Soc. China* **2016**, *26*, 1919–1925. [CrossRef]
37. Feng, X.-T.; Chen, S.; Zhou, H. Real-time computerized tomography (CT) experiments on sandstone damage evolution during triaxial compression with chemical corrosion. *Int. J. Rock Mech. Min. Sci.* **2004**, *41*, 181–192. [CrossRef]
38. Khandelwal, M.; Ranjith, P. Study of crack propagation in concrete under multiple loading rates by acoustic emission. *Geomechan. Geophys. Geo-Energy Geo-Resour.* **2017**, *3*, 393–404. [CrossRef]

© 2018 by the authors. Licensee MDPI, Basel, Switzerland. This article is an open access article distributed under the terms and conditions of the Creative Commons Attribution (CC BY) license (http://creativecommons.org/licenses/by/4.0/).